

Figure S1. Whole blot images for Figure 2E.

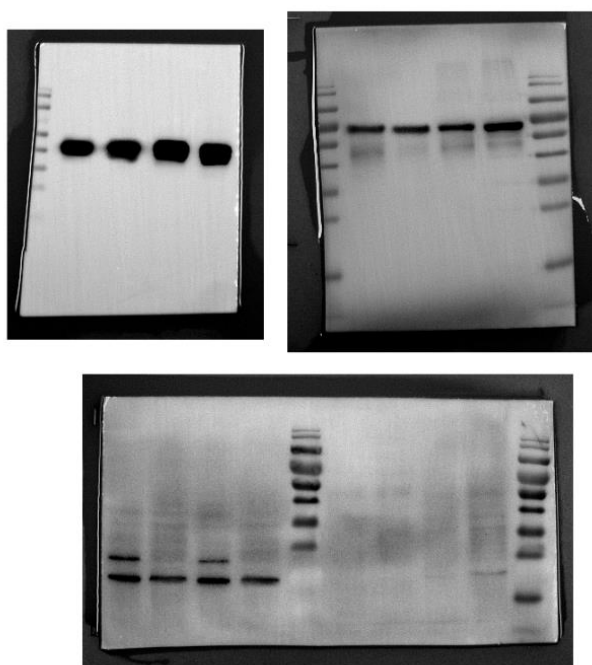


Figure S2. Whole blot images for Figure 3E.

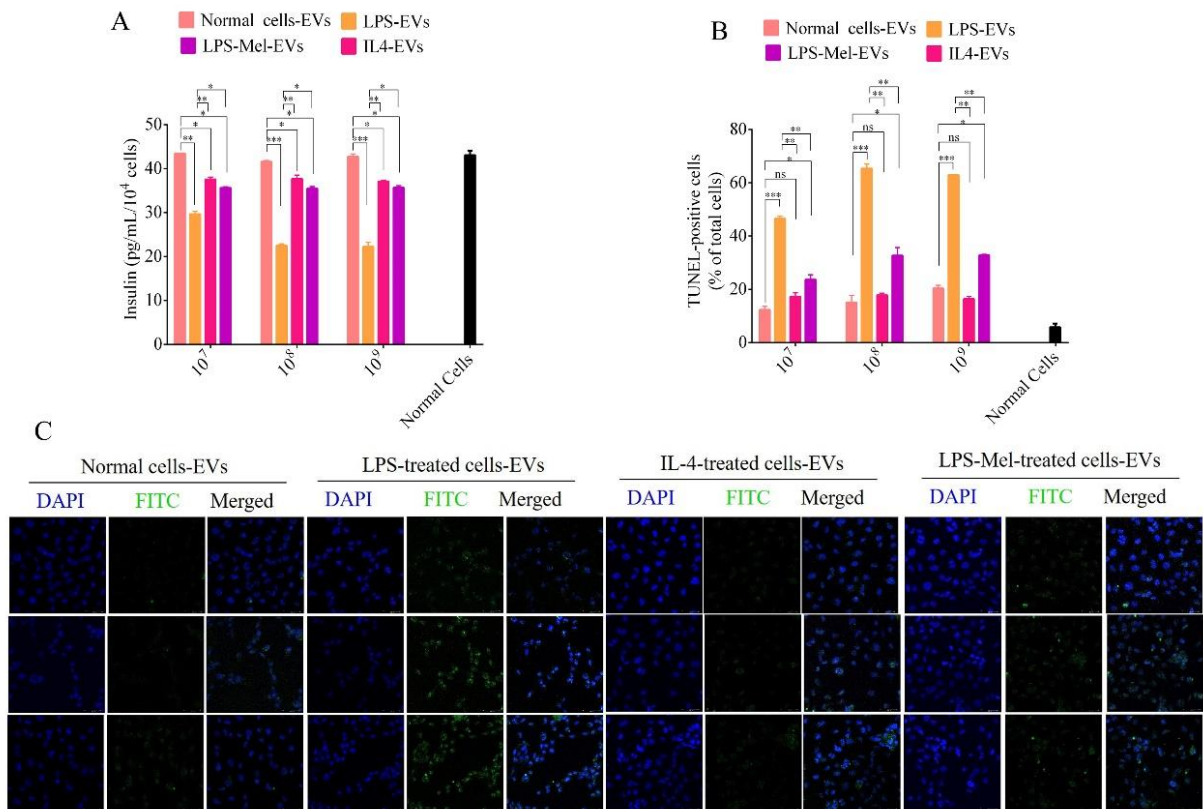


Figure S3. The role of EVs derived from PRMs, M1 phenotype PRMs, M2 phenotype PRMs and melatonin treated M1 phenotype. A. the analysis of insulin secretion of Beta TC-6 cells after treatment by various concentration EVs derived from pancreatic tissue. The insulin content in cellular supernatant from Beta TC-6 cells incubated with tissue EVs and then treatment with 20 mM glucose were detected by ELISA. B. Quantification analysis of the TUNEL-positive cells after treatment with various concentration EVs in Beta TC-6 cells. C. Representative fluorescent images of TUNEL staining after treatment with various concentration EVs in Beta TC-6 cells. (n=5). ns, not significant, * $P < 0.05$, ** $P < 0.01$, *** $P < 0.001$.

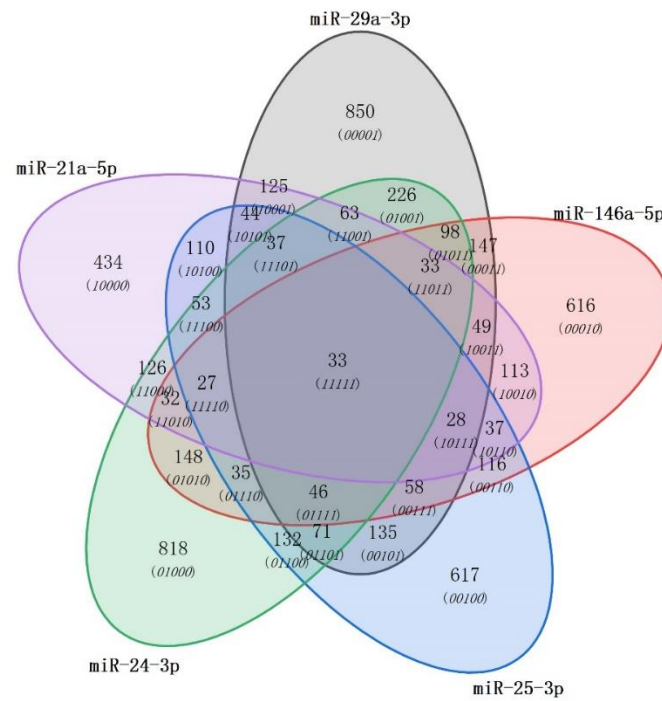


Figure S4. The target genes of miR-146a-5p, miR-29a-3p, miR-21-5p, miR-24-3p, and miR-25-3p are compared in a Venn diagram. Predicted target genes common to miRNAs were listed in Table S2.

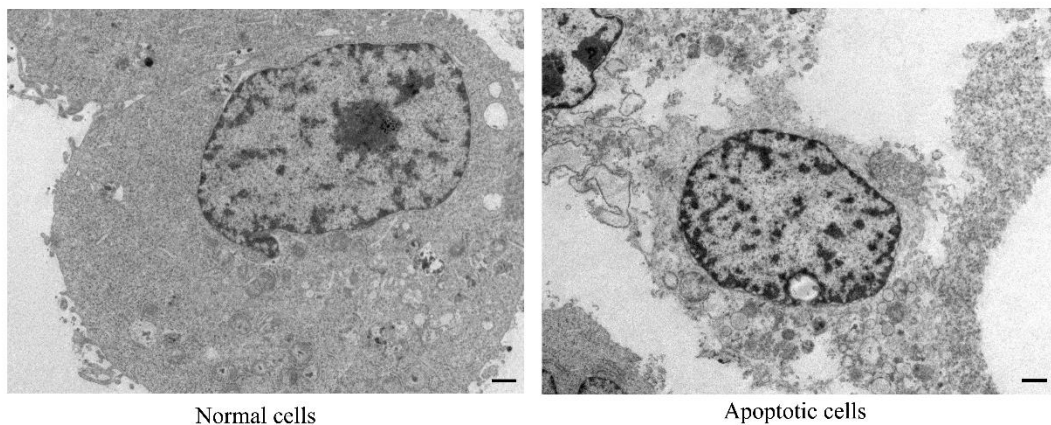


Figure S5. Electron microscopy images of β cells before and after various treatments.

Apoptotic bodies was observed in β cells after treatment with LPS-Exo, exosomes from IL-4-treated PRMs (IL-4-Exo), or exosomes from melatonin and LPS-treated PRMs (LPS-Mel-Exo) combined with specific miRNAs.

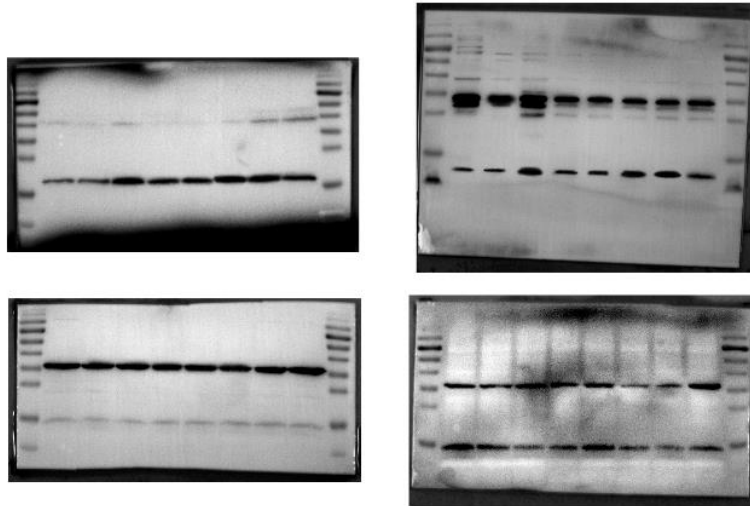


Figure S6. Whole blot images for Figure 4D.

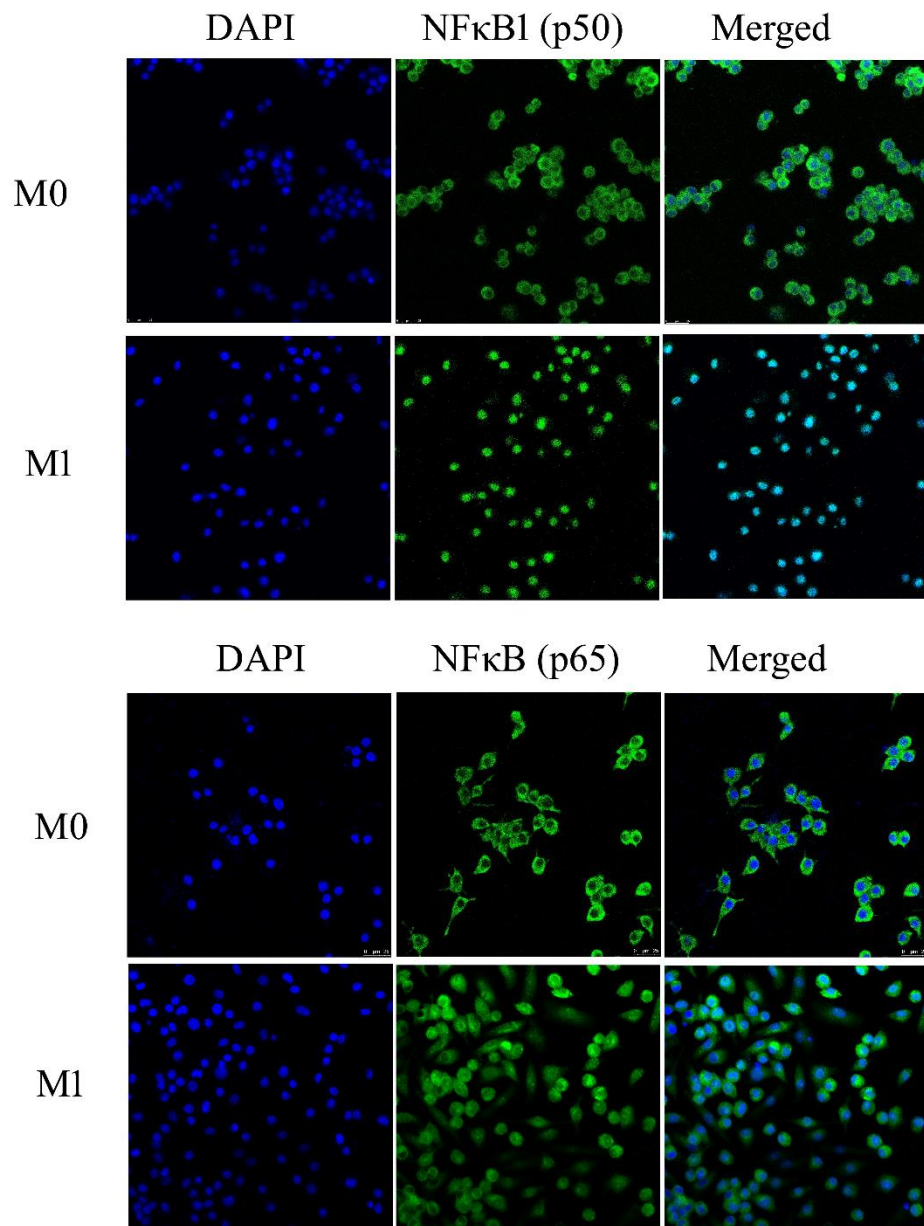


Figure S7. The immunofluorescence analysis of NF-κB (p65) and NF-κB (p50) were detected in PRMs after M1 polarization.

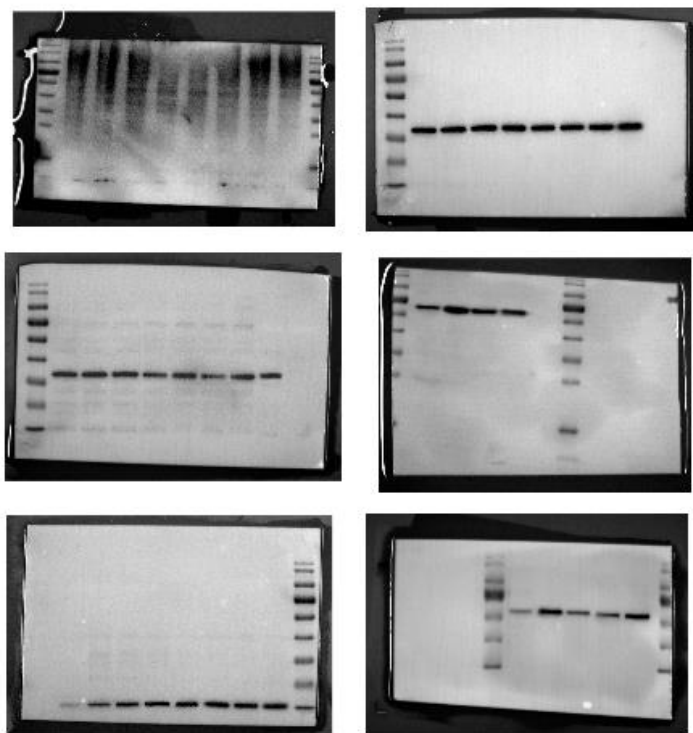


Figure S8. Whole blot images for Figure 5 A and B.

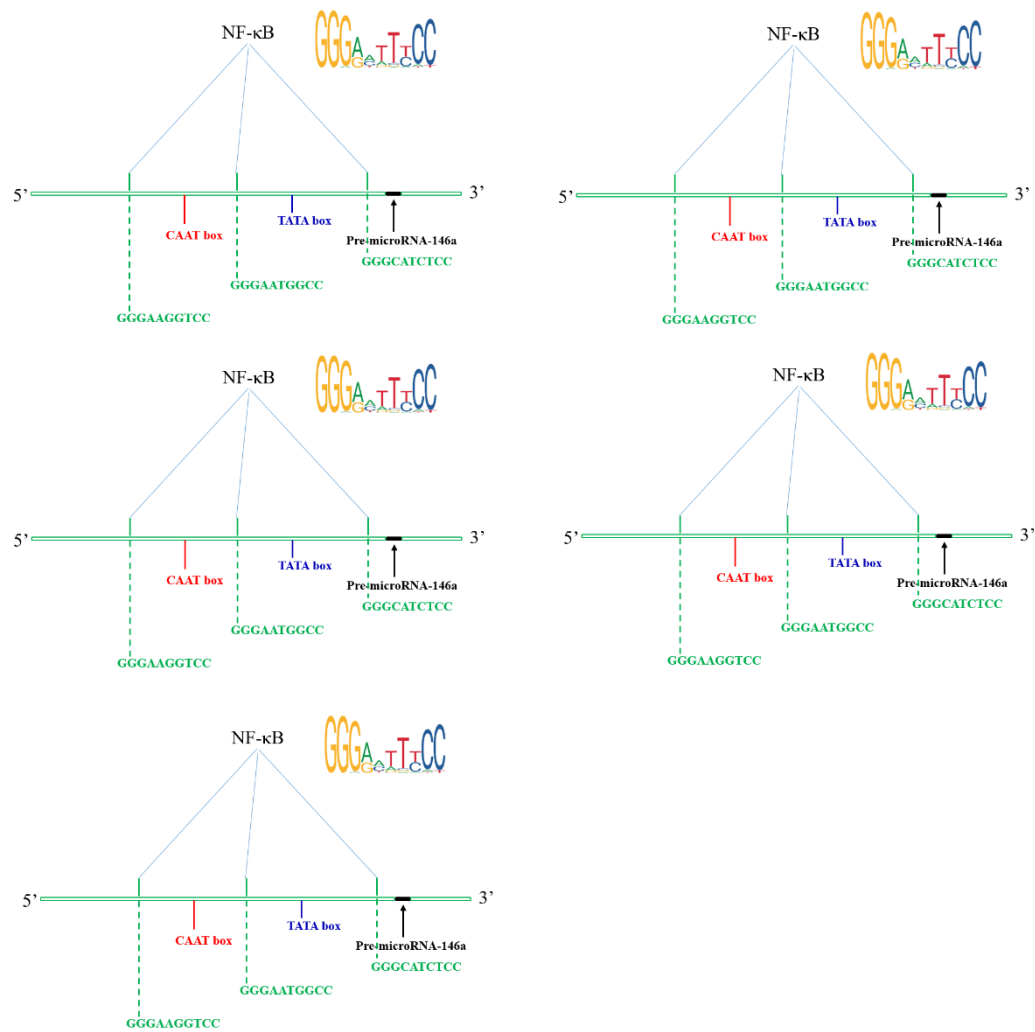


Figure S9. Schematic of the predicted binding sites of p50 transcription factors in the promoter regions of specific miRNAs. We used bioinformatic algorithms to screen for binding sites of p50 transcription factors within the 3 kbp upstream region of pre-miRNAs.

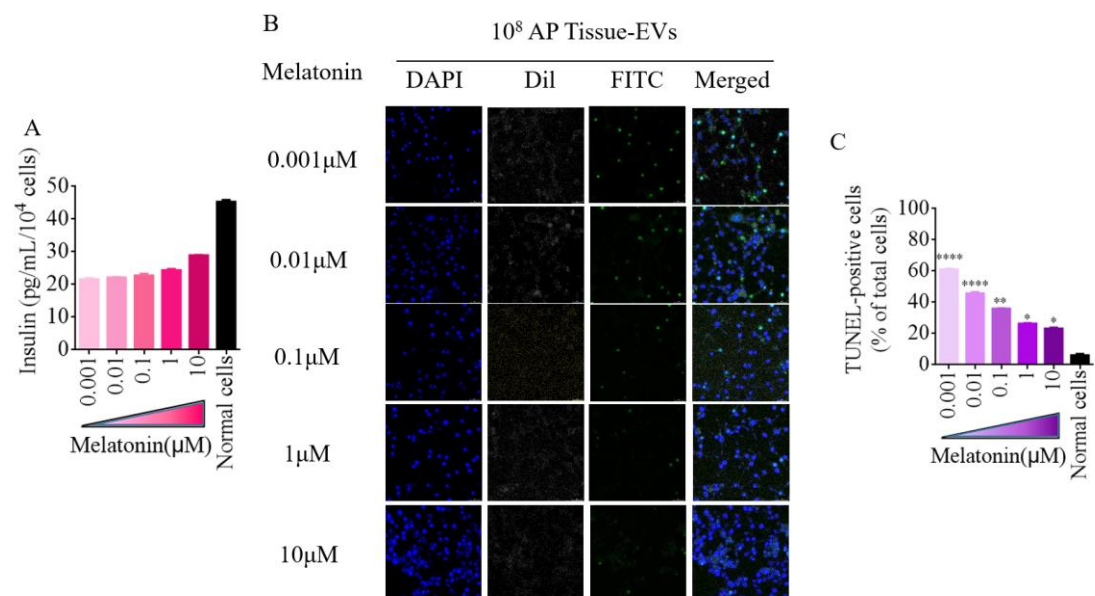
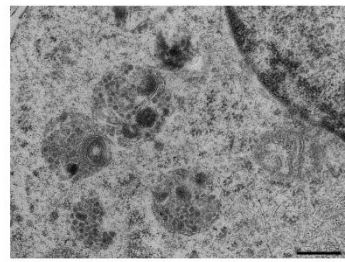
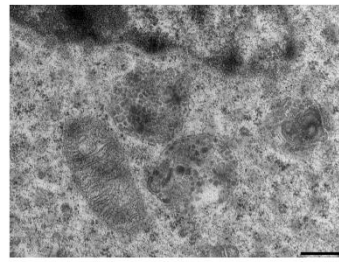


Figure S10. Melatonin effectively reduced cell apoptosis, and improved the insulin secretion with the increasing of melatonin concentration. A. the analysis of insulin secretion of Beta TC-6 cells after treatment by various dose melatonin. B. Representative fluorescent images of TUNEL staining after treatment with various dose melatonin in Beta TC-6 cells. C. Quantification analysis of the TUNEL-positive cells after treatment with various dose melatonin in Beta TC-6 cells. (n=5). ns, not significant, *P < 0.05, **P < 0.01, ***P < 0.001.



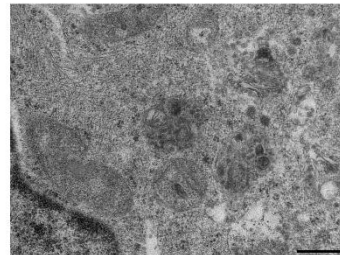
—



Normal cells-Exo



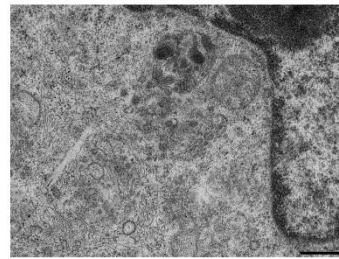
LPS-Exo



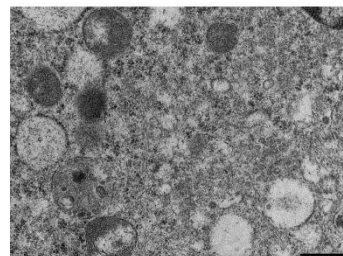
IL-4-Exo



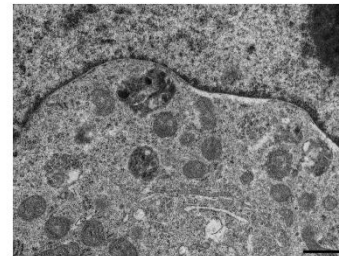
LPS-Mel-Exo



LPS-Mel-Exo+miRs



Normal cells-Exo+miRs



LPS-Exo+miRs inhibitor

Figure S11. Representative electron microscopy images of granules in β cells before and after various treatments.

Table S1 miRNA sponge sequence

Mature miRNA sequence		Sponge binding sites	
		Sense	Anti-sense
miR-24-3p	5'UGGCUCAGUUCAGCAGGAACAG	5'CTGTTCTGCCTTCTGAGCCA	5'TGGCTCAGAAGGCAGGAACAG
miR-25-3p	5'CAUUGCACUUGUCUCGGUCUGA	5'TCAGACCGAGGTTGTGCAATG	5'CATTGCACAACCTCGGTCTGA
miR-21-3p	5'UAGCUUAUCAGACUGAUGUUGA	5'TCAACATCAGGACATAAGCTA	5'TAGCTTATGTCCTGATGTTGA
miR-29a-3p	5'UAGCACCAUCUGAAAUCGGUUA	5'TAACCGATTTCTTGTTGCTA	5'TAGCACCAAGAAAATCGGTTA

Sponge sequence

Sense: 5' GTCC CTGTTCTGCCTTCTGAGCCA CCGG TCAGACCGAGGTTGTGCAATG CCGG TCAACATCAGGACATAAGCTA CCGG TAACCGATTTCTTGTTGCTA CCGG CTGTTCTGCCTTCTGAGCCA CCGG TCAGACCGAGGTTGTGCAATG CCGG TCAACATCAGGACATAAGCTA CCGG TAACCGATTTCTTGTTGCTA GG 3'

Anti-sense: 5' GACCC TAGCACCAAGAAAATCGGTTA CCGG TAGCTTATGTCCTGATGTTGA CCGG CATTGCACAACCTCGGTCTGA CCGG TGGCTCAGAAGGCAGGAACAG CCGG TAGCACCAAGAAAATCGGTTA CCGG TAGCTTATGTCCTGATGTTGA CCGG CATTGCACAACCTCGGTCTGA CCGG TGGCTCAGAAGGCAGGAACAG GG 3'